SUBMITTED ONLY

Mon. Not. R. Astron. Soc. 000, 1–5 (1998) Printed 13 July 1998 (MN LATEX style file v1.4)

An infrared image of the dust disc around β Pic ⋆

I. Heinrichsen [1,2†], H. J. Walker[3], U. Klaas[4,2], R. J. Sylvester[5], D. Lemke[4]

[1] *Max-Planck-Institut für Kernphysik, Saupfercheckweg 1, D-69117 Heidelberg, Germany*
[2] *ISO Science Operations Centre, Astrophysics Division of ESA, Space Science Department, VILSPA, P.O. Box 50727, E28080 Madrid, Spain*
[†] *Present address: IPAC, MS:100-22, California Institute of Technology, Pasadena, CA 91125, USA*
[3] *CLRC, Rutherford Appleton Laboratory, Chilton, Didcot, Oxon, OX11 0QX, UK*
[4] *Max-Planck-Institut für Astronomie, Königstuhl 17, D-69117 Heidelberg, Germany*
[5] *Dept. of Physics & Astronomy, University College, Gower Street, London, WC1E 6BT, UK*

Accepted Received

ABSTRACT

The star, β Pictoris, is a normal main sequence star with a remnant disc of cool dust around it. We present observations of the β Pic dust disc in the far infrared, obtained using the photometer (ISOPHOT) on the Infrared Space Observatory (ISO) satellite. We resolve the edge-on disc using high resolution scans, with a Full-Width-Half-Maximum of $8.7'' \pm 1.5''$ at 25μm (corresponding to a characteristic radius of 84AU) and $14.5'' \pm 2.0''$ at 60μm (corresponding to 140AU). The disc is just resolved in the minor axis direction at 60μm, with FWHM of $6.1'' \pm 2.0''$. Photometry, from 4.85μm to 200μm, is combined with low resolution spectroscopy and modelled to give an average dust temperature of 85K, using a blackbody modified by an emissivity proportional to λ^{-1}. A simple radiative transfer model is also used, with the grain radius ranging from 1μm to 1mm. The dust mass is estimated to be around (0.3 to 8) $\times 10^{-7}$ $M_\odot$, depending on the selected grain parameters.

Key words: circumstellar matter – infrared: stars – individual: β Pic

1 INTRODUCTION

The star β Pictoris is a main sequence star (A5V), known to be surrounded by a disc of dust which emits thermal radiation in the infrared (Gillett, 1986). Following the discovery with IRAS, the disc was imaged in scattered light at optical wavelengths by Smith and Terrile (1984) and others, and found to be edge-on. More recently the disc has been imaged in the near infrared by Mouillet et al (1997). Transient spectral signatures of infalling gas have been detected, which have been attributed to comets evaporating whilst falling onto the star by Lagrange-Henri et al (1988). Observations in the submm by Holland et al (1998) have also resolved the disc, with a deconvolved size of 22 × 11 (± 3) arcsec at 850μm. By observing the dust in the infrared (and submm), we can directly measure the disc properties, deriving the size and mass of the dust. The mass is found to be small, of the order of the lunar mass rather than the earth mass.

⋆ Based on observations with ISO, an ESA project with instruments funded by ESA Member States (especially the PI countries: France, Germany, the Netherlands and the United Kingdom) and with the participation of ISAS and NASA

2 OBSERVATIONS

Observations of the β Pic dust disc in the far infrared were obtained using the photometer (ISOPHOT) (Lemke et al, 1996) on the Infrared Space Observatory (ISO) satellite (Kessler et al, 1996). The photometric and spectroscopic observations were taken as part of the ISOPHOT guaranteed time programme, and the high spatial resolution linear scans resulted from a special solicited ISO proposal, dedicated to the detailed investigation of β Pic. Calibration observations and observations of the background near β Pic were taken around the same time.

ISOPHOT is a unique instrument, able to resolve the edge-on disc using high resolution scans, due to the excellent pointing accuracy of ISO (around 1″). At 25μm a set of eight scans were performed, at various angles to the major axis of the edge-on dust disc (see Fig. 1 and Table 1). Four scans were made at 60μm (see Table 1), along the major and minor axes and at two intermediate angles. The step size was 2″ at 25μm and 5″ at 60μm, making full use of the ISO pointing accuracy. Apertures were selected to match the step size and resolution; 10″ at 25μm (diffraction limit Full-Width-Half-Maximum (FWHM) 8″) and 23″ at 60μm (diffraction limit FWHM 19.2″). The scans at 25μm were entered using the Calibration Uplink System instead of the normal observing templates (AOTs) because the step between sampling points

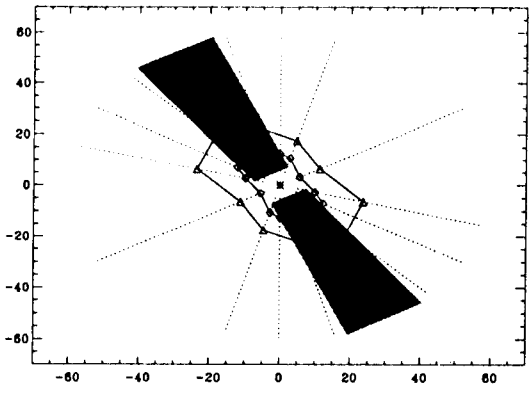

Figure 1. The orientations of the scans at 25μm (8 scans) are compared to a sketch of the disc parameters derived from the optical data. The distances are measured in arcsecs. The length of the dashed line shows the derived 5σ extent of the thermal disc from the infrared data. The measured (before deconvolution) Full-Width-Half-Maximum values for the disc of β Pic at 25μm (diamonds), and 60μm (triangles) are also given.

Table 1. Disc sizes from ISOPHOT high resolution scans

Wavelength (μm)	Angle (°)	Gaussian (″)	FWHM (″)
60	30	12.4	14.5
	75	9.8	11.5
	120	5.2	6.1
	165	7.3	8.6
25	0	5.0	5.9
	15	6.7	7.9
	30	7.4	8.7
	45	6.6	7.7
	60	5.6	6.6
	75	4.1	4.8
	120	2.5	2.9
	165	4.4	5.2

The disc is orientated at 30°, hence the scan made with ISO at 30° is along the major axis of the disc. The error is ± 2″ at 60μm and ± 1.5″ at 25μm.

was smaller than that allowed with AOTs. The full scan length was 56″ at 25μm and 140″ at 60μm. The disc is orientated at 30°, hence the scan made with ISO at 30° is along the major axis of the disc. Identical scans were made of HR6705 (γ Dra), a point source calibration reference star.

3 DATA REDUCTION

The data were reduced from Edited Raw Data (ERD) level using the ISOPHOT Interactive Analysis Software Package (PIA) † version 6.5 (Gabriel et al, 1996). The calibration is based on the general calibration files, version 3.1. Standard corrections for Cold-Readout-Electronics non-linearity, de-glitching and signal derivation were applied. The impact of detector transients was minimised using drift detection. The data were converted into flux density units (Jy) using the Fine Calibration Source (FCS) calibration. After background subtraction the 9 pixels of the C100 camera (60 – 100 μm) were added up and the result corrected for the point spread function of the array. The data of the individual pointings of the C200 camera (120 – 200 μm) mini-maps were extracted and an average background flux derived, subtracted, and finally the value of the centre pixel was used to derive the flux again taking into account the point spread function factor.

The same processing steps were applied to the low resolution spectroscopic data from 2.5μm to 5μm and 5.8μm to 11.6μm (taken with the PHT-S sub-instrument) as for the analysis of the photometric observations. However, the standard calibration file for converting the detector output signal into Jy (the spectral response function of PHT-S) was found to be inadequate for the flux range of β Pic. Therefore, we used the "dynamical spectral response correction" (Klaas et al, 1997). The calibration star HR6817 (K1III) was found to have the appropriate signal level over almost the full wavelength range of PHT-S, so the spectral response function was constructed from the average of 10 observations of this star. Only for the longest wavelengths where β Pic showed a rising spectrum, and HR6817 continued to fall, was there some mismatch in signal transient behaviour (resulting in a less satisfactory correction for the 9 to 11 μm region). The lower signal-to-noise of HR6817 in this wavelength range might also contribute to the flux discrepancy.

As the calibration for the short-wavelength detector (4.85 – 16 μm), using the FCS, did not yield satisfactory results, a special calibration procedure was performed using the same technique as was applied to the PHT-S data. Calibration observations of HR7341 (K1III) and HR7633 (K5II-III) were used, since these had similar flux densities to β Pic in the detector wavelength range.

The uncertainty in the flux density, estimated at wavelengths up to (and including) 16μm, was 30%. The uncertainty in the flux density, estimated at wavelengths beyond 16μm, was 20%.

4 RESULTS

4.1 Scans

The high resolution scan data were modelled assuming the intensity distribution from the dust was Gaussian in form, and so a Gaussian beam profile could be removed. This simple deconvolution gave the Gaussian width (at 60% of the peak signal) for each linear scan, and the FWHM was calculated from this (see Table 1). The value derived at 30° represents the maximum extent of the disc (the characteristic radius).

Fig. 2 shows the measured profiles (at 60μm) of β Pic at 30° and of HR6705, together with their Gaussian models,

† PIA is a joint development by the ESA Astrophysics Division and the ISOPHOT Consortium led by the Max Planck Institute for Astronomy (MPIA), Heidelberg. Contributing ISOPHOT Consortium institutes are DIAS, RAL, AIP, MPIK, and MPIA.

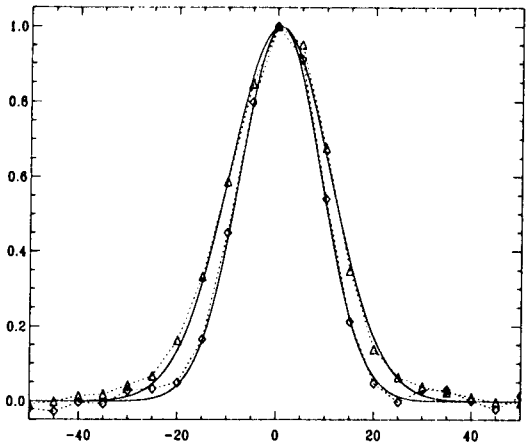

Figure 2. A scan along the disc of β Pic at 60μm, with position angle 30° (shown with triangles), compared with the scan across HR6705 (used as the point spread function), shown with diamonds. The Gaussians used for HR6705 and the model fit to β Pic are also shown with solid lines. The x-axis scale is in arcsecs, and the y-axis scale is flux density normalised to the peak value for each target.

to demonstrate the validity of this approach. Our value, at 60μm, for the FWHM of 14.5″ ± 2.0″ is smaller than the value (20″) derived by Gillett (1986) from IRAS data, who used the same simple deconvolution technique, and smaller than the value found by Holland et al (1998) in the submm. However, the value is in good agreement with that from Backman and Paresce (1993) of 13″. Gillett was not able to resolve the disc along the minor axis with IRAS, we find a FWHM of 6.1″ ± 2.0″ at 120°. Holland et al did not resolve the disc along the minor axis, in the submm. At 25μm the FWHM at 30° is 8.7″ ± 1.5″, and we have almost resolved the disc along its minor axis, with 2.9″ ± 1.5″ at 120° (see Fig. 1 and Table 1). The minor axis size is smaller than the value derived from optical data. The minor-to-major axis ratio gives a minimum inclination angle (assuming zero thickness) of 65° at 60μm and 71° at 25μm.

The polar diagram of the disc dimensions from the scans (expressed as FWHM) is given in Fig. 1. The sizes given from optical data typically measured the full extent at zero intensity. Smith and Terrile (1984) gave 60″ as the radius of the dust disc seen in scattered light, more recent work by Kalas and Jewitt (1995) gives 40″ to 48″. To compare this with the value we derive from the Gaussian width (σ), we use a 5σ level to indicate the edge of the disc. The size of the disc from optical data is larger than the 5σ value from our infrared data, which gives a radius of 31″ at 60μm, the peak of the thermal emission from the dust.

Using a smooth local thin plate spline interpolation (Franke, 1982), the eight calibrated high resolution scans were mapped onto a 512×512 grid, using the individual positions (in astronomical coordinates) as reconstructed from the ISO satellite data, for both β Pic and HR6705 (a calibration star) representing the beam profile. The bottom panel shows the result of 100 iterations of the maximum entropy deconvolution (Hollis et al, 1992) of β Pic by HR6705. It

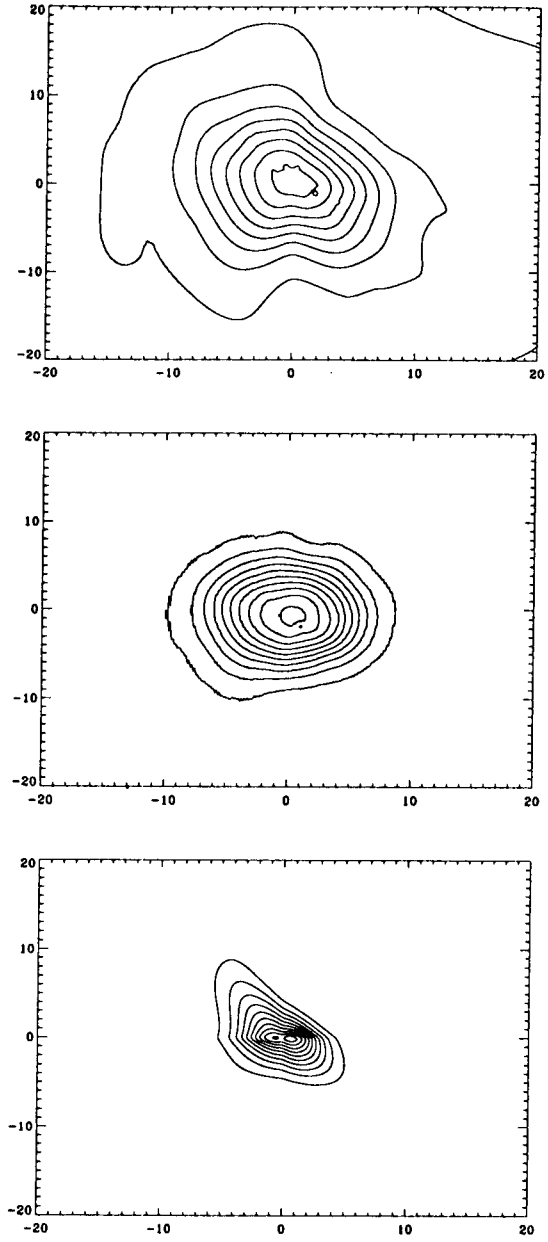

Figure 3. Contour plots (40″ × 40″) constructed from the scan data at 25μm. The raw images of β Pic (top) and HR6705 (a calibration star) representing the beam profile (middle) are shown. The bottom panel gives the result of the deconvolution of β Pic by HR6705. There are 10 contour levels shown in each panel, evenly spaced between the maximum and minimum flux density values.

suggests that there is a warp in the inner disc with respect to the disc major axis, and an asymmetry with respect to the NE direction. This warp is similar to that seen in the scattered light images from HST (at optical wavelengths), and an asymmetry was predicted at 20μm by Pantin et al (1997), from a model based on data at 10μm. Kalas and Jewitt (1995) describe five types of asymmetry from their R

Table 2. ISOPHOT Photometry of β Pic

λ_c (μm)	Flux (Jy)		cc Flux (Jy)
4.85	5.3	± 1.6	5.1
7.3	3.2	± 1.0	2.8
11.3	2.8	± 0.8	2.8
12.8	3.2	± 1.0	3.2
16	2.5	± 0.8	2.6
20	8.7	± 1.8	8.9
25	10.2	± 2.0	10.5
60	18.5	± 3.7	17.0
80	17.8	± 3.6	12.4
100	9.4	± 1.9	7.4
120	7.7	± 1.6	5.1
150	4.8	± 1.0	3.6
170	4.1	± 0.8	2.5
200	1.8	± 0.4	1.7

Each flux density is colour corrected using either adjacent data points (from 4.85μm to 16μm) or with an 85K blackbody (from 20μm).

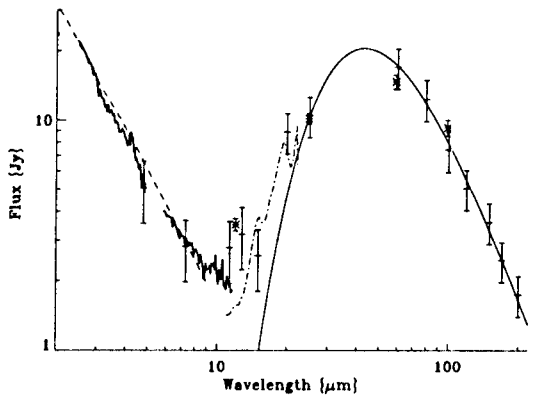

Figure 4. The spectral energy distribution of β Pic. ISOPHOT photometric data are shown as crosses, the IRAS data as asterisks. The ISO PHT-S low resolution spectrum from 2.5μm to 5μm and 5.8μm to 11.6μm is shown as a solid line. The thin dot-dash line gives the smoothed IRAS LRS spectrum of β Pic from the LRS database. The dashed line from 1μm to 9μm shows the Kurucz model. The solid curve from 15μm to 200μm shows the model for the thermal dust emission, with a blackbody of T=85K modified by an emissivity law of $Q(\lambda) \propto \lambda^{-1}$. The short dash line shows the radiative transfer model, which used silicate grains with sizes between 1μm and 1mm.

band data, some of which can be explained by the scattering geometry.

4.2 Photometry

Table 2 shows the flux densities derived for β Pic from the ISOPHOT photometric data, from 4.85μm to 200μm. The table also gives the values after colour correction (shown in Fig. 4).

The ISOPHOT photometry agrees well with the IRAS photometry. The stellar properties of β Pic have been re-analysed in the light of the new distance (19.28 ± 0.19 pc) from Hipparcos (Crifo et al, 1997). ¿From 2.5μm to around 9μm the PHT-S data and the two photometric data points (at 4.85μm and 7.3μm) can be interpreted as pure photospheric emission, and they are well represented by a Kurucz (1992) model, with T_{eff}=8500K and log g=4.5, absolutely calibrated using $L/L_\odot$=8.9, $R/R_\odot$=1.46, and the Hipparcos distance (19.28pc). The far infrared photometry shows the thermal emission from the dust, which is represented by a blackbody of 85K modified by an emissivity law $Q(\lambda) \propto \lambda^{-1}$. The model predicts a flux of 36mJy at 800μm, which agrees with the upper limit from Zuckerman and Becklin (1993) of 80mJy, but is significantly lower than the flux found at 850μm by Holland et al (1998). The model predicts 10mJy at 1300μm, again it is lower than the value of 24.9±2.6mJy determined by Chini et al (1991). Fig. 4 also shows a simple radiative transfer model, using silicate grains with sizes ranging from 1μm to 1mm. The ISOPHOT and IRAS data between 8μm and 20μm show that there is an additional emission component, a mixture of thermal emission (with a temperature between around 300K and 500K) and silicate dust emission observed by Knacke et al (1993) (shown here by the rise in emission from 9μm to 11.6μm in Fig. 4). Emission by polycyclic aromatic hydrocarbons (PAHs) can be excluded, due to the lack of emission features at 7.7μm and 11.3μm. Li and Greenberg (1998) modelled the silicate feature using cometary dust models.

5 DISCUSSION

The flux in the cool (85K) dust component is 6.5×10^{25} W (which corresponds to $0.17L_\odot$), so $L_{FIR}/L_* = 0.019$, which is higher than earlier estimates. The warm component (between 10μm and 23 μm) contains 3.3×10^{25} W ($0.09L_\odot$). Klaas and Elsässer (1993) used the far infrared luminosity and dust temperature to estimate dust mass, for β Pic we derive the dust mass to be 8×10^{-7} $M_\odot$ (or $20M_{moon}$). The dust mass can be estimated, using the slightly different assumptions of Becklin and Zuckerman (1990) to be 3×10^{-8} $M_\odot$ ($0.9M_{moon}$). This range in mass shows that the mass is very dependent on the assumptions used in the modelling, and in particular on the particle size distribution. The value of $7.8M_{moon}$ found from submm observations (Holland et al, 1998) falls within this range. The critical grain radius, using Backman and Paresce (1993), is estimated to be 2.3μm. The radiative transfer model using silicate grains with sizes between 1μm and 1mm gives a reasonable fit to the far infrared photometry and scan data, for a dust mass of 4.4×10^{-8} $M_\odot$, and with an inner cavity of radius 0.67 AU. Single power laws were used to describe the grain size and spatial density distributions. The model underestimates the flux in the 10μm region: a more elaborate density distribution function is needed to match the observed flux over the full region of excess emission.

The critical grain radius for β Pic is much smaller than that derived with ISOPHOT data for Vega of 110μm (Heinrichsen et al, 1997), and the dust mass is larger ($0.3 - 1.5 \times 10^{-8} M_\odot$ for Vega, from Heinrichsen et al). β Pic is younger than Vega, very close to (or on) the Zero-Age-Main-Sequence, according to Crifo et al (1997). The results for β Pic are in general agreement with earlier work, although the derived dust mass is lower. The high resolution scans at

60μm give a characteristic radius of 140AU for the disc, with a minor axis height of 59AU. At 25μm, the characteristic radius is 84AU (the disc height is not resolved). These values are very similar to the values Heinrichsen et al (1997) found for Vega. We expect the characteristic radius at 25μm to be smaller than that at 60μm, since the warmer material will be closer to the star. This may also account for the larger radius in the submm, in that the submm will again sample a cooler dust population. The fact that the two stars give the same characteristic radius at 60μm, despite the different distances to the stars, reflects the peak emission of dust heated by an A star, and does not exclude the presence of cooler dust at greater distances.

The upper limit to the 'grain' radius is not constrained by the infrared data. The dust mass range derived here is more similar to typical disc masses expected around main sequence stars (Beckwith and Sargent, 1996) than earlier estimates, which suggested a range of dust mass from $3 \times 10^{-6}M_{\odot}$ (for an upper limit to the grain radius of 1mm) to $1.5 \times 10^{-5}M_{\odot}$ (for an upper limit of 100km - the size of an asteroid), from Leinert and Grün (1990). When our dust mass is combined with the interstellar gas-to-dust ratio (100) the total mass in the disc could be as high as $10^{-4}M_{\odot}$ (or larger if β Pic has a significant number of asteroids in the disc). However, it is unlikely that the gas-to-dust ratio is that high, since the gas emission features are transient (Lagrange-Henri et al, 1988). The mass of the interplanetary dust in our own solar system is estimated to be $<10^{20}$g ($5 \times 10^{-14}M_{\odot}$), equivalent to one large comet (Leinert and Grün, 1990), however, the mass of material in the Oort cloud is uncertain. The warp in the disc and the relatively frequent occurrence of material falling on to the star (Lagrange-Henri et al 1988), suggests that the β Pic system is more perturbed than our solar system. Li and Greenberg (1998) model the 10μm silicate feature with cometary-type dust, including crystalline silicate dust. The Poynting-Robertson drag and radiation pressure show that dust grains should have been removed from the β Pic system (Wolstencroft and Walker, 1988), but the disc is continually replenished from a disc of comets around the star, similar to the Oort cloud around our own solar system. The dust mass derived from submm observations is within the range of the dust mass derived using several models for the infrared data, which suggests that, although the very cool dust may have a larger physical disc radius, it does not contain a significant amount of material.

ACKNOWLEDGMENTS

The Strasbourg Astronomical Data Centre (CDS) SIMBAD database has been used for the catalogue and literature research. We are grateful to the other members of the ISOPHOT Instrument Dedicated Team, P. Richards (RAL) and P. Ábrahám (MPIA) for their support and useful discussions. One of us (HJW) is very grateful to MPIA for their hospitality during the summer of 1997.

REFERENCES

Backman, D. E. and Paresce, F., 1993, In 'Protostars & Planets III', eds. E. H. Levy and J. I. Lunine (U. of Arizona, Tuscon), p. 1253.

Becklin, E. E. and Zuckerman, B., 1990, In 'Submillimetre Astronomy' eds. G. D. Watt and A. S. Webster (Kluwer, Dordrecht), p. 147.

Beckwith, S.V.W. and Sargent, A.I., 1996, Nature 383, 139.

Chini, R., Krügel, E., Shustov, B., Tutukov, A. and Kreysa, E., 1991, Astron. Astrophys. 252, 220.

Crifo, F., Vidal-Madjar, A., Lallement, R., Ferlet, R. and Gerbaldi, M., 1997, Astron. Astrophys. 320, L29.

Franke, R., 1982, Computer Math with Applications 8, 273.

Gabriel, C., et al, 1996, In 'ADASS VI, Conference on Astronomical Data Analysis Software and Systems' (Charlottesville, USA).

Gillett, F. C., 1986, In 'Light on Dark Matter' ed. F. P. Israel (Reidel, Dordrecht), p. 61.

Heinrichsen, I., Walker, H.J. and Klaas, U., 1997, Mon Not. R. Astron. Soc. 293, L78.

Holland, W.S., Greaves, J.S., Zuckerman, B., Webb, R.A., McCarthy, C., Coulson, I.M., Walther, D.M., Dent, W.R.F., Gear, W.K., Robson, I., 1998, Nature 392, 788.

Hollis, J.M., Dorband, J.E. and Yusef-Zadeh, F., 1992, Astrophys. J. 386, 293.

Kalas, P. and Jewitt, D., 1995, Astron. J. 110, 794.

Kessler, M. F., Steinz, J. A., Anderegg, M. E., et al, 1996, A&A 315, L27.

Klaas, U., Acosta-Pulido, J.A., Ábrahám, P. et al, 1997, In 'Proceedings of first ISO workshop on analytical spectroscopy', ESA SP-419, p. 113.

Klaas, U. and Elsässer, H., 1993, A&A 280, 76.

Knacke, R.F., Fajardo-Acosta, S.B., Telesco, C.M., Hackwell, J.A., Lynch, D.K. and Russell, R.W., 1993, Astrophys. J. 418, 440.

Kurucz, R.L., 1992, In 'The stellar populations of galaxies', eds. B. Barbuy and A. Renzini (Kluwer, Dordrecht), p. 225.

Lagrange-Henri, A.M., Vidal-Madjar, A. and Ferlet, R., 1988, Astron. Astrophys. 190, 275.

Leinert, Ch. and Grün, E., 1990, In 'Physics of the inner heliosphere I', Space and Solar Physics Vol. 20, eds R. Schwenn and E. Marsch (Springer, Berlin).

Lemke, D., Klaas, U., Abolins, J., et al, 1996, Astron. Astrophys. 315, L64.

Li, A. and Greenberg, J.M., 1998, Astron. Astrophys. 331, 291.

Mouillet, D., Lagrange, A.-M., Beuzit, J.-L., Renaud, N., 1997, Astron. Astrophys. 324, 1083.

Pantin, E., Lagage, P.O. and Artmowicz, P., 1997, Astron. Astrophys. 327, 1123 (1997).

Smith, B.A. and Terrile, R.T., 1984, Science 226, 1421.

Wolstencroft, R.D. and Walker, H.J., 1988, Phil. Trans. R. Soc. London A 325, 423.

Zuckerman, B. and Becklin, E. E., 1993, ApJ 414, 793.

This paper has been produced using the Royal Astronomical Society/Blackwell Science LaTeX style file.